S^3 Skyrmions and the Rational Map Ansatz

S Krusch[*]

Department of Applied Mathematics and Theoretical Physics
University of Cambridge
Wilberforce Road, Cambridge CB3 0WA, England

June 19, 2000

Abstract

This paper discusses multi-Skyrmions on the 3-sphere S^3 with variable radius L using the rational map ansatz. For baryon number $B = 3, \ldots, 9$ this ansatz produces the lowest energy solutions known so far. By considering the geometry of the model we find an approximate analytic formula for the shape function. This provides an insight why Skyrmions have a shell-like structure.

PACS-number: 12.39.Dc

27 pages, 14 figures

---

[*]email: S.Krusch@damtp.cam.ac.uk

1 Introduction

In this paper we discuss new developments in the $SU(2)$ Skyrme model [1] and its generalization to the case where the physical space is a 3-sphere of radius L. The Skyrme model is a nonlinear field theory of mesons whose field configurations are labelled by an integer, the topological charge. This charge can be identified with the baryon number B [1]. Static field configurations which minimize the energy of the Skyrme model for a given baryon number B are called Skyrmions. When the theory is quantized, the Skyrme model not only describes the proton and the neutron reasonably well [2, 3] but also larger nuclei [4, 5]. However, in order to be able to perform the quantization it is important to reach a good understanding of the classical solutions. In [6] Skyrmions were calculated numerically for small baryon number B, and it was shown that they have certain discrete symmetries. These symmetries have been confirmed by the rational map ansatz [7] which also reproduces the energies of the Skyrmions with good accuracy.

From a mathematical point of view, field configurations in the Skyrme model are represented by maps from $(\mathbb{R}^3 \cup \{\infty\}) \cong S^3$ to $SU(2) \cong S^3$. Therefore, it is natural to generalize the model such that physical space is a 3-sphere of radius L. From a physical point of view, a Skyrmion on a 3-sphere describes a finite baryon density [8]. Reducing L increases the baryon density. Varying L the S^3 model exhibits phenomena such as localization–delocalization transitions and the restoration of chiral symmetry. These results can be compared with Skyrme crystal calculations [9, 10, 11], but are also interesting in their own right.

In this paper we only consider static configurations and their energies. In particular, we generalize the rational map ansatz to describe Skyrmions on S^3. The energies of our ansatz are the lowest ones known so far. Moreover, these approximations have a well defined limit for $L \to \infty$, namely, the rational map Skyrmions in flat space. Geometric considerations lead to an analytic ansatz for the shape function which is completely specified by a small set of parameters. We show that this ansatz agrees well with the numerical solution and captures the behaviour of Skyrmions on S^3.

In the following section we review the Skyrme model on general 3-dimensional manifolds. The first part focuses on the geometrical meaning of the Skyrme energy. The next part clarifies the relationship between the geometric formulation in flat space and the standard formulation in terms of the Lie group $SU(2)$. In section 3 the model is generalized to the 3-sphere. We describe the rational map ansatz in detail and also recall the doubly axially-symmetric ansatz [12]. In section 4 we derive an analytic ansatz for the shape function and discuss its symmetries. For special values of B the energy can be calculated explicitly as a function of the radius L. In section 5 we calculate the shape function numerically. We also compare the numerical shape function to the analytic shape function of the previous section. Finally, we use the analytic shape function to approximate Skyrmions in $\mathbb{R}^3$. In section 6 we discuss chiral symmetry and phase transitions.

2 Geometry of Skyrmions

In this section we describe static solutions of the Skyrme model on general 3-dimensional manifolds. We follow Manton's approach [8] and present a geometric point of view. First, we introduce the geometric notion of the strain tensor and construct the Skyrme energy for general manifolds. Then we discuss the properties of the energy density and derive some formulae which will be important in the following sections. Finally, we show that in flat space the geometric energy density is equivalent to the standard energy density.

A field configuration is a map π from a physical space S to a target space Σ. Both S and Σ are 3-dimensional Riemannian manifolds which are connected and orientable, and their metrics are t_{ij} and $\tau_{\alpha\beta}$, respectively. We denote by x a point in S and $\pi(x)$ its image in Σ. Choosing dreibeins $e_m{}^i(x)$ on S and $\zeta_\mu{}^\alpha(\pi(x))$ on Σ, we can define the Jacobian matrix

$$J_{m\mu}(x) = e_m{}^i(x)(\partial_i\pi^\alpha(x))\zeta_{\mu\alpha}(\pi(x)). \tag{2.1}$$

The matrix $J_{m\mu}(x)$ is a measure of the deformation induced by the map π at the point x in S. However, it is not unique since a rotation of the dreibeins $\zeta_\mu{}^\alpha(\pi(x))$ does not affect the geometrical deformation. This leads us to define the strain tensor

$$D_{mn} = (JJ^T)_{mn} = e_m{}^i(\partial_i\pi^\alpha)e_n{}^j(\partial_j\pi^\beta)\tau_{\alpha\beta} \tag{2.2}$$

which only depends on the metric on Σ. Here and in the following we suppress the direct reference to x. The strain tensor is symmetric and positive semi-definite[1] but it is not invariant under rotation of the dreibeins $e_m{}^i$. In fact, under an orthogonal transformation O, D transforms into O^TDO. A well known result from linear algebra is that the characteristic polynomial $P(\lambda) = \det(D - \lambda I)$ is invariant under orthogonal transformations. Denoting the non-negative eigenvalues of the strain tensor D by λ_1^2, λ_2^2, and λ_3^2 we obtain the following invariants of D:

$$\text{Tr } D = \lambda_1^2 + \lambda_2^2 + \lambda_3^2$$

$$\tfrac{1}{2}(\text{Tr } D)^2 - \tfrac{1}{2}\text{Tr } D^2 = \lambda_1^2\lambda_2^2 + \lambda_2^2\lambda_3^2 + \lambda_1^2\lambda_3^2 \tag{2.3}$$

$$\det D = \lambda_1^2\lambda_2^2\lambda_3^2.$$

As we will demonstrate in this section, choosing the energy of a field configuration to be the integral of the following sum of these invariants generalizes the Skyrme model to arbitrary manifolds S and Σ:

$$E = \int_S \lambda_1^2 + \lambda_2^2 + \lambda_3^2 + \lambda_1^2\lambda_2^2 + \lambda_2^2\lambda_3^2 + \lambda_1^2\lambda_3^2 \tag{2.4}$$

where the integration measure is $\sqrt{\det t}\ \mathrm{d}^3x$. The first three terms are only quadratic in the derivatives and correspond to the "sigma model term". The configurations which are

---

[1] Generically, J is non-degenerate so that D is positive definite. However, there are submanifolds of zero baryon density, i.e. $\det(J(x)) = 0$. For further discussion see [13].

minimizing this term are known as harmonic maps [14]. Geometrically, π induces a linear map π^* mapping the unit vector $e_m{}^i$ which is formed by the mth dreibein to the vector $e_m{}^i \partial_i \pi^\alpha$. The sum of the squared lengths of these vectors is the "sigma model term". Thus, only the lengths of the vectors $\pi^*(e_m{}^i)$ are important.

The geometric meaning of the quartic terms can be understood by considering the area element $\epsilon^{qmn} e_m{}^i e_n{}^j$ formed by two dreibeins. This area element is mapped to the following area element in Σ:

$$\epsilon^{qmn} e_m{}^i e_n{}^j \partial_i \pi^\alpha \partial_j \pi^\beta. \tag{2.5}$$

The sum of the squares of these area elements is proportional to the "Skyrme term". This term is also a measure of the angular distortion of the map π^*.

So far only the first two invariants of the strain tensor have been used. The third invariant is the square of the determinant of the Jacobian, $(\det J)^2$. Since the manifolds S and Σ are orientable, $\det J$ is globally well defined so that we can set $\sqrt{\det D} = \det J$. $\det J$ locally changes the integration measure on S into the measure on Σ. Therefore, the integral of $\det J$ over S is equal to the volume $\mathrm{Vol}(\Sigma)$ times the degree of the map π. The degree of a map is a topological invariant which, roughly speaking, measures how many preimages a point $\pi(x)$ of Σ has in S, and hence takes integer values. Any field configuration can be labelled by its degree. In the Skyrme model the degree of the map π is identified with the baryon number B, and we obtain

$$B = \frac{1}{\mathrm{Vol}(\Sigma)} \int_S \lambda_1 \lambda_2 \lambda_3. \tag{2.6}$$

We will call classical field configurations which minimize the energy (2.4) Skyrmions. It is worth pointing out that there is an alternative expression for equation (2.4). By "completing the square" we can rearrange the λ_i in the following way:

$$E = \int_S (\lambda_1 \pm \lambda_2 \lambda_3)^2 + (\lambda_2 \pm \lambda_3 \lambda_1)^2 + (\lambda_3 \pm \lambda_1 \lambda_2)^2 \mp 6\lambda_1 \lambda_2 \lambda_3. \tag{2.7}$$

Either the upper or the lower signs are chosen such that the integral over the last term in equation (2.7) is non-negative. Applying equation (2.6), this integral is just $6\,|B|\,\mathrm{Vol}(\Sigma)$. Therefore, the energy is bounded below by the so-called Faddeev-Bogomolny bound [15]:

$$E \geq 6\,|B|\,\mathrm{Vol}(\Sigma). \tag{2.8}$$

Equation (2.7) also gives rise to two sets of three Bogomolny equations which are satisfied if and only if the Faddeev-Bogomolny bound is attained,

$$\lambda_1 = \mp \lambda_2 \lambda_3, \ \ \lambda_2 = \mp \lambda_3 \lambda_1 \ \ \text{and} \ \ \lambda_3 = \mp \lambda_1 \lambda_2. \tag{2.9}$$

The only non-trivial solutions of both sets of equations are $\lambda_1^2 = \lambda_2^2 = \lambda_3^2 = 1$, and it follows that $B = \lambda_1 \lambda_2 \lambda_3 = \mp 1$. Therefore, the strain tensor is the identity map, and the map π is an isometry. For $\Sigma = SU(2)$, this case can only occur if the physical space is a 3-sphere of radius $L = 1$. This has already been proven in [16].

The relative importance of the "sigma model term" and the "Skyrme term" can be seen from their scaling behaviour. For this purpose we consider a family of metrics $L^2 t_{ij}$ where L is a constant length scale. The dreibeins $e_m{}^i$ are, informally speaking, the square roots of the inverse metric $\frac{1}{L^2} t^{ij}$ of S. Therefore, they are proportional to $\frac{1}{L}$ so that the eigenvalues λ_i^2 of the strain tensor D_{ij} are proportional to $\frac{1}{L^2}$. Since the measure $\sqrt{\det(L^2 t_{ij})}\, \mathrm{d}^3 x$ scales with L^3, the "sigma model term" scales like L, whereas the Skyrme term scales like $\frac{1}{L}$. For large radius L one might expect the "sigma model term" to be dominant. Yet, this is not the case because, as we shall see, the Skyrmion becomes localized and — just as in flat space — both of these terms are equally important. However, for small radius L the configuration is delocalized, and the "Skyrme term" will become dominant.

In the following, we relate this geometric formulation to the standard Skyrme model in flat space. For the remainder of this section S will correspond to the flat space $\mathbb{R}^3$ and Σ to the Lie group $SU(2) \cong S^3$. The basic field is the $SU(2)$ valued field

$$U(\mathbf{x}) = \sigma(\mathbf{x}) + i\boldsymbol{\pi}(\mathbf{x}) \cdot \boldsymbol{\tau} \tag{2.10}$$

where τ_i are the Pauli matrices which are Hermitian and satisfy the algebra $\tau_i\tau_j = \delta_{ij} + i\epsilon_{ijk}\tau_k$. Since U is an element of $SU(2)$, the fields σ and $\boldsymbol{\pi}$ obey the constraint $\sigma^2 + \boldsymbol{\pi}^2 = 1$. It is worth noting that $\boldsymbol{\pi}$ in (2.10) play the same role as the coordinates π_i in the discussion above, and σ is just a function of those coordinates. The static solutions of the Skyrme model can be derived by varying the following energy [7]:

$$E = \int \left(-\frac{1}{2}\mathrm{Tr}\,(R_i R_i) - \frac{1}{16}\mathrm{Tr}\,([R_i, R_j][R_i, R_j]) \right) \mathrm{d}^3\mathbf{x} \tag{2.11}$$

where $R_i = (\partial_i U)U^\dagger$ is an $su(2)$ valued current. A static solution of the variational equations could also be a saddle point. Only solutions which minimize the energy are called Skyrmions. In order to show that the energies (2.4) and (2.11) are equivalent, we first relate the strain tensor D_{ij} to the current R_i. Since σ is determined by $\boldsymbol{\pi}$ we can calculate the induced metric $\tau_{\alpha\beta}$ on the target space Σ in terms of the fields $\boldsymbol{\pi}$:

$$\tau_{\alpha\beta} = \delta_{\alpha\beta} + \frac{\pi_\alpha \pi_\beta}{\sigma^2}. \tag{2.12}$$

Starting from equation (2.2) and noting that in flat space the dreibeins can be chosen to

be Kronecker deltas we obtain the following expression:

$$D_{ij} = \partial_i \pi^\alpha \partial_j \pi^\beta \tau_{\alpha\beta} \tag{2.13}$$

$$= \partial_i \sigma \partial_j \sigma + \partial_i \boldsymbol{\pi} \cdot \partial_j \boldsymbol{\pi} \tag{2.14}$$

$$= \frac{1}{2} \mathrm{Tr} \left((\partial_i \sigma + i\boldsymbol{\tau} \cdot \partial_i \boldsymbol{\pi})(\partial_j \sigma - i\boldsymbol{\tau} \cdot \partial_j \boldsymbol{\pi}) \right) \tag{2.15}$$

$$= \frac{1}{2} \mathrm{Tr} \left(\partial_i U \partial_j U^\dagger \right) \tag{2.16}$$

$$= -\frac{1}{2} \mathrm{Tr} \left(R_i R_j \right). \tag{2.17}$$

Equation (2.14) follows from (2.13) by using the chain rule and the formula for the metric (2.12). Conceptually, the step from equation (2.14) to equation (2.15) is very important. The metric $\tau_{\alpha\beta}$ is expressed with the group multiplication and the trace which provides a scalar product in $su(2)$. This is the transition from geometric to Lie group language. Equation (2.16) is a trivial consequence of definition (2.10), and the last equation follows from $UU^\dagger = 1$. Now, we can show that the two energy densities are equal. Since R_i is an $su(2)$ current, and therefore anti-Hermitian, it can be expressed as $R_i = R_i^\alpha \, i\tau_\alpha$. We start with the energy density in (2.11) and expand R_i in terms of Pauli matrices:

$$-\frac{1}{2}\mathrm{Tr} \left(R_i^\mu R_i^\nu i\tau_\mu i\tau_\nu \right) - \frac{1}{16}\mathrm{Tr} \left(R_i^\mu R_j^\nu [i\tau_\mu, i\tau_\nu] R_i^{\mu'} R_j^{\nu'} [i\tau_{\mu'}, i\tau_{\nu'}] \right) \tag{2.18}$$

$$= R_i^\mu R_i^\mu + \frac{1}{4}\mathrm{Tr} \left(R_i^\mu R_j^\nu \epsilon_{\mu\nu\rho} \tau_\rho R_i^{\mu'} R_j^{\nu'} \epsilon_{\mu'\nu'\rho'} \tau_{\rho'} \right) \tag{2.19}$$

$$= D_{ii} + \frac{1}{2} \left(R_i^\mu R_i^\mu R_j^\nu R_j^\nu - R_i^\mu R_j^\mu R_i^\nu R_j^\nu \right) \tag{2.20}$$

$$= D_{ii} + \frac{1}{2} \left(D_{ii} D_{jj} - D_{ij} D_{ji} \right) \tag{2.21}$$

$$= \mathrm{Tr}\ D + \frac{1}{2} \left(\mathrm{Tr}\ D \right)^2 - \frac{1}{2}\mathrm{Tr}\ D^2. \tag{2.22}$$

Equation (2.19) follows from (2.18) by inserting the commutation relations of the Pauli matrices $\boldsymbol{\tau}$. In the following equation we use the contraction $\epsilon_{ijk}\epsilon_{ilm} = \delta_{jl}\delta_{km} - \delta_{jm}\delta_{kl}$. In equation (2.21) we apply the result (2.17). The last equality follows from the definition of the trace. Equation (2.22) is the energy (2.4) because of (2.3). Therefore, we have shown the equivalence of the two approaches for $S = \mathbb{R}^3$. It is worth noting that in the geometric picture the "Skyrme term" is related to the square of an area element, whereas in the standard approach it depends on the structure constants of the Lie algebra $su(2)$. Both interpretations lead to generalizations. While in our geometric interpretation it is natural

5

to consider different 3-dimensional manifolds for S, and maybe for Σ, the Lie algebra approach leads to generalizing the Lie group $SU(2)$ for example to $SU(N)$.

3 Skyrmions on S^3 and Rational Maps

In the previous section we have established the equivalence of the two energies (2.4) and (2.11) in $\mathbb{R}^3$. In this section we will use (2.4) to generalize the model to $S = S_L^3$ such that from now on physical space is a 3-sphere of radius L. This includes the original model if we take the limit $L \to \infty$. We also fix $\Sigma = SU(2) \cong S_1^3$.

The Skyrme model cannot be solved analytically either in flat space, or on S_L^3, apart from the case if $L = 1$ and $B = 1$ as mentioned above. However, in flat space there are analytic ansätze which give good qualitative and quantitative agreement with exact solutions obtained numerically. By ansatz we mean a test function that minimizes the energy within a given class of test functions. The lower the energy the better we expect the ansatz to approximate the exact solution. In the following we will generalize the rational map ansatz [7], which has been very successful in flat space, to S_L^3.

A rational map is a holomorphic function from $S^2 \to S^2$. Treating each S^2 as a Riemann sphere, with complex coordinates z and R, respectively, a rational map can be written as

$$R(z) = \frac{p(z)}{q(z)} \tag{3.1}$$

where $p(z)$ and $q(z)$ are polynomials in z which are assumed to have no common factors. It has been shown by Donaldson [17], and also by Jarvis [18], that there is a one-to-one correspondence between rational maps and monopoles. In flat space it has been found that many solutions of the Skyrme equation with baryon number B look rather like monopoles with monopole number equal to B. Therefore, rational maps can be used to approximate Skyrmions.

A point x on S_L^3 is labelled by polar coordinates (μ, θ, ϕ) such that

$$x = (L\sin\mu\sin\theta\cos\phi, L\sin\mu\sin\theta\sin\phi, L\sin\mu\cos\theta, L\cos\mu) \tag{3.2}$$

$$= (L\sin\mu\,\hat{\mathbf{n}}(\theta,\phi), L\cos\mu) \tag{3.3}$$

where μ, $\theta \in [0, \pi]$, and $\phi \in [0, 2\pi]$ and $\hat{\mathbf{n}}(\theta,\phi)$ is the unit vector on S^2. The 3-sphere can be thought of as a collection of 2-spheres with varying radius equal to $L\sin\mu$. With the stereographic projection $z = \tan\frac{\theta}{2}e^{i\phi}$ the S^2 can be identified with a Riemann sphere using a single complex coordinate z. Alternatively, we can express the unit vector $\hat{\mathbf{n}}$ in terms of z:

$$\hat{\mathbf{n}}(z) = \frac{1}{1+|z|^2}\left(2\mathrm{Re}(z), 2\mathrm{Im}(z), 1 - |z|^2\right). \tag{3.4}$$

Similarly, points in the target S^3 can be labelled by (f, R) where f is an angular variable analogous to μ, and R is a complex coordinate. The rational map ansatz simply states

that $f = f(\mu)$ and $R = R(z)$. This is only consistent if $\sin f(\mu)$ vanishes where $\sin \mu$ does, i.e. $f(0) = N_1 \pi$ and $f(\pi) = N_2 \pi$. The integer $N_f = N_1 - N_2$ is a topological invariant and cannot be changed by deforming $f(\mu)$ smoothly. In order to have a good limit for $L \to \infty$ we fix $f(\mu)$ such that $N_2 = 0$ and set $N_1 = N_f$. In analogy to flat space we define a Skyrmion to have $N_f > 0$, whereas for an anti-Skyrmion $N_f < 0$. Since Skyrmions and anti-Skyrmions are related by reflection we will only consider Skyrmions from now on. Therefore, our complete boundary conditions are:

$$f(0) = N_f \pi \quad \text{where} \quad N_f > 0$$

$$f(\pi) = 0. \tag{3.5}$$

In contrast to the flat case these boundary conditions do not follow from a regularity argument. They are an artifact of our ansatz and have to be handled with care (see [19] for a discussion).

If we now use the notation of equation (2.10) we can write the Skyrme field in the following way:

$$U(\mu, z, \bar{z}) = \cos f(\mu) + i \ \sin f(\mu) \ \hat{\mathbf{n}}(R(z)) \cdot \boldsymbol{\tau} \tag{3.6}$$

$$= \exp\left(i \ f(\mu) \ \hat{\mathbf{n}}(R(z)) \cdot \boldsymbol{\tau}\right) \tag{3.7}$$

where $\hat{\mathbf{n}}(R(z))$ is as in equation (3.4). Equation (3.7) looks quite similar to the well known spherically symmetric hedgehog ansatz [1]. In fact, the hedgehog ansatz corresponds to the special case $R(z) = z$.

Now, we can apply the formulae of the previous section. The rational map ansatz gives rise to the following eigenvalues λ_i^2 of the strain tensor (2.2):

$$\lambda_1 = -\frac{f'}{L} \quad \text{and} \quad \lambda_2 = \lambda_3 = \frac{\sin f}{L \sin \mu} \frac{1 + |z|^2}{1 + |R|^2} \left| \frac{\mathrm{d}R}{\mathrm{d}z} \right|. \tag{3.8}$$

The minus sign in the expression for λ_1 is a consequence of our definition of positive baryon number in (3.5). One advantage of the rational map ansatz is the decoupling of the radial and the angular strains. Starting from formula (2.6) the baryon number B can be written as a product of two integrals, one over μ and one over z and $\bar{z}$ in the following way:

$$B = \frac{2}{\pi} \int \left(-f' \sin^2 f\right) \mathrm{d}\mu \ \frac{1}{4\pi} \int \left(\frac{(1 + |z|^2)}{(1 + |R|^2)} \left| \frac{\mathrm{d}R}{\mathrm{d}z} \right|\right)^2 \frac{2i \ \mathrm{d}z \mathrm{d}\bar{z}}{(1 + |z|^2)^2} \tag{3.9}$$

$$= N_f N_R. \tag{3.10}$$

The integral over μ is the integer N_f. The second integral is the pull-back of the area form on the target sphere of the rational map $R(z)$. Taking the normalization into account this is just the degree N_R of the rational map $R(z)$. In fact, it can be shown that if $p(z)$ has the degree n_p and $q(z)$ has the degree n_q then $N_R = \max(n_p, n_q)$.

7

The energy can now be obtained from formula (2.4):

$$E = \int \left[\frac{f'^2}{L^2} + 2\left(\frac{f'^2}{L^2} + 1\right) \frac{\sin^2 f}{L^2 \sin^2 \mu} \left(\frac{1+|z|^2}{1+|R|^2} \left|\frac{\mathrm{d}R}{\mathrm{d}z}\right|\right)^2 \right. \tag{3.11}$$

$$\left. + \frac{\sin^4 f}{L^4 \sin^4 \mu} \left(\frac{1+|z|^2}{1+|R|^2} \left|\frac{\mathrm{d}R}{\mathrm{d}z}\right|\right)^4 \right] \frac{2i \, \mathrm{d}z\mathrm{d}\bar{z}}{(1+|z|^2)^2} L^3 \sin^2 \mu \, \mathrm{d}\mu.$$

Similarly to the baryon density, the integration over z and $\bar{z}$ and the integration over μ factorizes. Therefore, formula (3.11) can be rewritten as

$$E = 4\pi \int \left(f'^2 L \sin^2 \mu + 2N_R(\frac{f'^2}{L} + L) \sin^2 f + \mathcal{I} \frac{\sin^4 f}{L \sin^2 \mu} \right) \mathrm{d}\mu \tag{3.12}$$

where N_R is the degree of the rational map, and $\mathcal{I}$ is the following special function on the space of rational maps:

$$\mathcal{I} = \frac{1}{4\pi} \int \left(\frac{1+|z|^2}{1+|R|^2} \left|\frac{\mathrm{d}R}{\mathrm{d}z}\right|\right)^4 \frac{2i \, \mathrm{d}z\mathrm{d}\bar{z}}{(1+|z|^2)^2}. \tag{3.13}$$

To minimize E for a given baryon number $B = N_f N_R$, one should first minimize $\mathcal{I}$ over the space of rational maps of degree N_R. This calculation was performed in [7], and the result is displayed in table 1 in the appendix. Then the profile function $f(\mu)$ is found by solving the following Euler-Lagrange equation:

$$f'' \left(\frac{2N_R}{L^2} \sin^2 f + \sin^2 \mu\right) + 2f' \sin \mu \cos \mu + \frac{2N_R}{L^2} f'^2 \sin f \cos f$$

$$- 2N_R \sin f \cos f - \frac{2\mathcal{I} \sin^3 f \cos f}{L^2 \sin^2 \mu} = 0 \tag{3.14}$$

where $\mathcal{I}$ now takes the constant value in table 1. We require $f(\mu)$ to be a solution of (3.14) non-singular in $[0, \pi]$. Equation (3.14) has to be solved numerically. It has regular singular points at the end points, *i.e.* close to these points the solution has the following power law behaviour: $f(\mu) \approx N_f \pi - A_{\pm} \mu^{\rho_{\pm}}$ for $\mu \approx 0$ and $f(\mu) \approx B_{\pm}(\pi - \mu)^{\rho_{\pm}}$ for $\mu \approx \pi$. Here $\rho_{\pm} = \frac{1}{2}(\pm\sqrt{1 + 8N_R} - 1)$ and $A_{\pm}$ and $B_{\pm}$ are arbitrary constants. The solution $f(\mu)$ is regular if the exponent is equal to ρ_+ at both end points.

Equation (3.12) has an important discrete symmetry. The transformation

$$f(\mu) \to N_f \pi - f(\pi - \mu) \tag{3.15}$$

transforms a solution of (3.14) into a solution which is also compatible with the boundary conditions (3.5). Geometrically, $\mu \to \pi - \mu$ is a reflection at the plane through the equator in physical space, whereas $f \to N_f \pi - f$ is a reflection in target space. This means that

8

a solution which is localized for example at the south pole $\mu = \pi$ is transformed to a solution which is localized at the north pole $\mu = 0$. Therefore, for fixed B there are two degenerate solutions unless the transformation (3.15) is a symmetry of $f(\mu)$ in which case there is only one symmetric solution. The symmetry (3.15) does not have an analogue in flat space. Also note that the transformations $f(\mu) \to f(\pi - \mu)$ and $f(\mu) \to -f(\mu)$ take a Skyrmion with baryon number B into an anti-Skyrmion with baryon number $-B$.

When we derived the energy of the rational map ansatz we used equation (2.4). This could be transformed into equation (2.7) by "completing the square". Having now calculated the integral over the rational map, we can complete the square in a different way and re-express (3.12) as

$$
E = 4\pi L \int_0^\pi \left[\left(f' \sin \mu + \frac{\sqrt{\mathcal{I}} \sin^2 f}{L \sin \mu} \right)^2 + 2 N_R \sin^2 f \left(\frac{f'}{L} + 1 \right)^2 \right] \mathrm{d}\mu
$$

$$
-8\pi (2 N_R + \sqrt{\mathcal{I}}) \int_0^\pi f' \sin^2 f \, \mathrm{d}\mu. \qquad (3.16)
$$

The second integral in (3.16) can be evaluated using $f(0) = N_f \pi$ and $f(\pi) = 0$. Since the first integral in (3.16) is positive the second integral provides us with the energy bound

$$
E \;\geq\; 4\pi^2 (\sqrt{\mathcal{I}} + 2 N_R) N_f \qquad (3.17)
$$

$$
\geq\; 12\pi^2 N_R N_f. \qquad (3.18)
$$

The last inequality is valid because $\mathcal{I} \geq N_R{}^2$ which can easily be shown by applying the Schwartz inequality. Therefore, inequality (3.17) "improves" the Faddeev-Bogomolny bound (2.8) where $\mathrm{Vol}(\Sigma) = 2\pi^2$ and $B = N_R N_f$. This rational map bound (3.17) is valid, if the fields obey the rational map ansatz. Exact solutions satisfy neither the rational map ansatz nor necessarily the bound (3.17). We will discuss this bound further in section 5.

Before ending this section we review one further ansatz. The symmetry group of S_L^3, which is $O(4)$, contains an $O(2) \times O(2)$ subgroup. Jackson *et al* used this symmetry to obtain doubly axially-symmetric ansätze for Skyrmions of various baryon numbers B [12]. In order to make best use of the symmetry it is convenient to parameterize the 3-sphere with a different set of angles (χ, α, β). With these coordinates a point on S_L^3 can be written as

$$
x = (L \sin \chi \cos \alpha, L \sin \chi \sin \alpha, L \cos \chi \cos \beta, L \cos \chi \sin \beta) \qquad (3.19)
$$

where $\chi \in [0, \frac{\pi}{2}]$ and $\alpha, \beta \in [0, 2\pi]$. Now we can write an $O(2) \times O(2)$ symmetric field configuration $U \in SU(2)$ as

$$
U = \sin g \cos p\alpha + i\tau_3 \sin g \sin p\alpha + i\tau_1 \cos g \cos q\beta + i\tau_2 \cos g \sin q\beta \qquad (3.20)
$$

where p and q are integers and $g = g(\chi)$ is a shape function. In this ansatz the eigenvalues λ_i of the strain tensor (2.2) are

$$
\lambda_1 = \frac{g'}{L}, \quad \lambda_2 = \frac{p \sin g}{L \sin \chi} \quad \text{and} \quad \lambda_3 = \frac{q \cos g}{L \cos \chi}. \qquad (3.21)
$$

9

Using equation (2.4) we obtain the energy

$$E = 2\pi^2 L \int \left(g'^2 + \frac{p^2 \sin^2 g}{\sin^2 \chi} + \frac{q^2 \cos^2 g}{\cos^2 \chi} \right) \sin(2\chi) \mathrm{d}\chi \tag{3.22}$$

$$+ \frac{2\pi^2}{L} \int \left(g'^2 \left(\frac{p^2 \sin^2 g}{\sin^2 \chi} + \frac{q^2 \cos^2 g}{\cos^2 \chi} \right) + \frac{p^2 q^2 \sin^2 g \cos^2 g}{\sin^2 \chi \cos^2 \chi} \right) \sin(2\chi) \mathrm{d}\chi$$

and the baryon number

$$B = pq \int 2g' \sin g \cos g \ \mathrm{d}\chi. \tag{3.23}$$

The shape function $g(\chi)$ can be calculated numerically by minimizing the energy E subject to the boundary conditions $g(0) = 0$ and $g(\frac{\pi}{2}) = \frac{\pi}{2}$ for various p, q and L. Note that these boundary conditions for $g(\chi)$ imply that $B = pq$. In [12] the energy for a given baryon number B was also minimized with respect to the radius L. Some of the results are displayed in figure 5 of section 5. It was shown that the solutions are only stable as long as L is smaller than a B-dependent critical length $L_{crit.}$. Moreover, for large baryon number B the minimal energy for the optimal radius L is larger than the energy of B well separated Skyrmions in $\mathbb{R}^3$. Therefore, in this situation the ansatz fails badly. However, for small baryon number B and small radius L the ansatz is quite successful. For $B = 1$ it agrees with the known $O(4)$ symmetric solution. For $B = 2$ it predicts an $O(2) \times O(2)$ symmetric solution with a very low energy. Given that the exact $B = 2$ solution in flat space possesses an $O(2) \times \mathbb{Z}_2$ symmetry this configuration is likely to be the exact solution on S^3.

One particular feature of configurations of the form (3.20) is that the following order parameter O_1 vanishes:

$$O_1 = \langle \sigma \rangle^2 + \langle \boldsymbol{\pi} \rangle^2 = 0 \tag{3.24}$$

where $\langle \ \rangle$ means the average over the physical S_L^3. It also turns out that configurations with $p = q$ attain their minimal energy at particularly small values of L. Moreover, for $p = q$ the solution has a symmetry similar to (3.15). The transformation

$$g(\chi) \rightarrow \frac{\pi}{2} - g(\frac{\pi}{2} - \chi) \tag{3.25}$$

transforms solutions of the Euler-Lagrange equation for the energy (3.22) into each other. We will need these properties in section 6.

4 The Shape Function as a Quasi-Conformal Map

We discuss next the shape function $f(\mu)$ of the rational map ansatz. Since solving equation (3.14) numerically provides little insight we derive an analytic shape function. This ansatz approximates the numerical shape function fairly accurately and also confirms geometric ideas.

In [8] Manton approximated the shape function of the $B = 1$ Skyrmion by a conformal map. With this ansatz he showed that a delocalized $B = 1$ Skyrmion on a 3-sphere is

unstable for $L > \sqrt{2}$. In this section we will generalize this idea for higher baryon number B. Using the rational map ansatz we will derive an ansatz for the shape function which is conformal in an average sense and which we will call quasi-conformal. In the following section, we will show that this quasi-conformal ansatz is a good approximation to the numerically calculated shape function.

A Skyrmion is a map from physical space S_L^3 labelled by (μ, z) to a target $S_1^3 \cong SU(2)$ labelled by (f, R). A map between two 3-spheres is conformal if their metrics only differ by a conformal factor:

$$L^2 \, \mathrm{d}\mu^2 + L^2 \, \sin^2 \mu \frac{2i \, \mathrm{d}z \, \mathrm{d}\bar{z}}{(1 + z\bar{z})^2} = \Omega(\mu, z, \bar{z})^2 \left(\mathrm{d}f^2 + \sin^2 f \frac{2i \, \mathrm{d}R \, \mathrm{d}\bar{R}}{(1 + R\bar{R})^2} \right). \tag{4.1}$$

We are interested in fields which obey the rational map ansatz, i.e. $f = f(\mu)$ and $R = R(z)$. Therefore, we make the following approximations to equation (4.1). Firstly, since $f(\mu)$ is a function of μ only, we consider a conformal factor Ω which is also only a function of μ. Secondly, we recall that according to equation (3.9) the integral over the target S^2 is just 4π times the degree N_R of the rational map. Therefore, we replace the metric on the target S^2 by N_R times the metric on the physical S^2. Locally, this is not a very good approximation, but averaged over the whole S^2 this reproduces the correct result. Since $f(\mu)$ is independent of z and $\bar{z}$ it can only detect the averaged value. With these approximations equation (4.1) can be simplified:

$$L^2 \, \mathrm{d}\mu^2 + L^2 \, \sin^2 \mu \frac{2i \, \mathrm{d}z \, \mathrm{d}\bar{z}}{(1 + z\bar{z})^2} = \Omega(\mu)^2 \left(\mathrm{d}f^2 + \sin^2 f \; N_R \frac{2i \, \mathrm{d}z \, \mathrm{d}\bar{z}}{(1 + z\bar{z})^2} \right). \tag{4.2}$$

Eliminating $\Omega(\mu)$ from equation (4.2) we obtain the following differential equation for $f(\mu)$:

$$\left(f'(\mu) \right)^2 \sin^2 \mu = N_R \sin^2 f(\mu). \tag{4.3}$$

We are interested in solutions which obey the boundary conditions (3.5). It is convenient to replace $\sin f(\mu)$ by $\sin(\pi - f(\mu))$ before taking the square root:

$$f'(\mu) \sin \mu = \pm \sqrt{N_R} \sin(\pi - f(\mu)). \tag{4.4}$$

For the negative sign the solution of equation (4.4) diverges at the boundary and can therefore be discarded. Equation (4.4) is solved by separation of variables, and we obtain

$$f(\mu) = \pi - 2 \arctan \left(k \left(\tan \frac{\mu}{2} \right)^{\sqrt{N_R}} \right) \tag{4.5}$$

where k is a positive integration constant. A negative k would lead to a negative baryon number and is incompatible with the boundary conditions (3.5) whereas $k = 0$ is just the trivial solution with baryon number $B = 0$. The quasi-conformal shape function (4.5) satisfies our boundary conditions (3.5) if and only if $N_f = 1$. With equation (3.10) we

obtain $B = N_R$. The shape function (4.5) has the following important property. Using the identity

$$\arctan x + \arctan \frac{1}{x} = \frac{\pi}{2} \quad \text{for} \quad x \geq 0 \tag{4.6}$$

it is easy to show that for $k = 1$ the shape function (4.5) is invariant under the discrete symmetry (3.15):

$$f(\mu) = \pi - f(\pi - \mu). \tag{4.7}$$

This means that for $k = 1$ the solution is neither localized at the south pole nor at the north pole. For $N_R = 1$ the solution is delocalized over the whole sphere whereas for $N_R > 1$ it is rather localized at the equator $\mu = \frac{\pi}{2}$. By Taylor expanding equation (4.5) near $\mu = 0$ we find that the shape function $f(\mu)$ behaves like $f(\mu) \approx \pi - 2k(\frac{\mu}{2})^{\sqrt{N_R}}$. Recall that for the exact solution of the Euler-Lagrange equation (3.14) we obtained $f(\mu) \approx \pi - A_+ \mu^{\rho_+}$ where $\rho_+ = -\frac{1}{2} + \frac{1}{2}\sqrt{1 + 8N_R}$. So at $\mu = 0$ the shape function (4.5) and the exact solution have a similar behaviour. The same is true for the other boundary $\mu = \pi$.

Now, we can substitute the shape function (4.5) into the equation for the energy (3.12) and obtain

$$E = 16\pi \left(3LN_R I_1(k) + \frac{4}{L} \left(2N_R{}^2 + \mathcal{I} \right) I_2(k) \right) \tag{4.8}$$

where

$$I_1(k) = \int_0^\infty \frac{2k^2 y^{2\sqrt{N_R}}}{(1 + k^2 y^{2\sqrt{N_R}})^2 (1 + y^2)} \mathrm{d}y \tag{4.9}$$
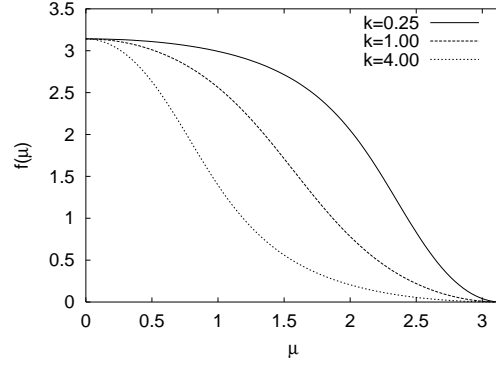
and

$$I_2(k) = \int_0^\infty \frac{k^4 y^{4\sqrt{N_R} - 2}(1 + y^2)}{2(1 + k^2 y^{2\sqrt{N_R}})^4} \mathrm{d}y. \tag{4.10}$$
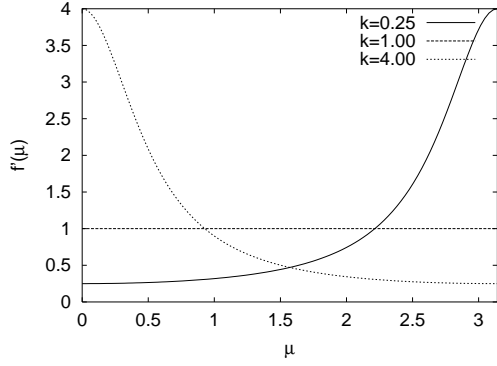
In (4.9) and (4.10) we have simplified the integrand by substituting $y = \tan \frac{\mu}{2}$. The integrals $I_1(k)$ and $I_2(k)$ can be evaluated in closed form if $\sqrt{N_R}$ is an integer. Therefore, we will concentrate on $N_R = 1$, 4 and 9 in the remainder of this section.
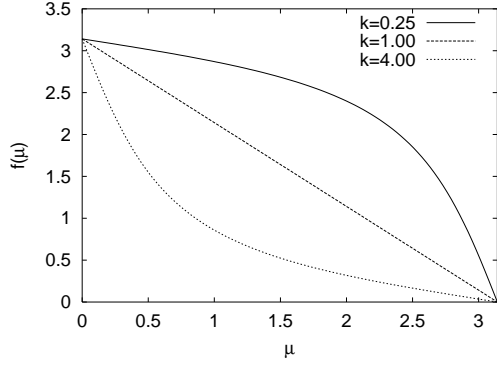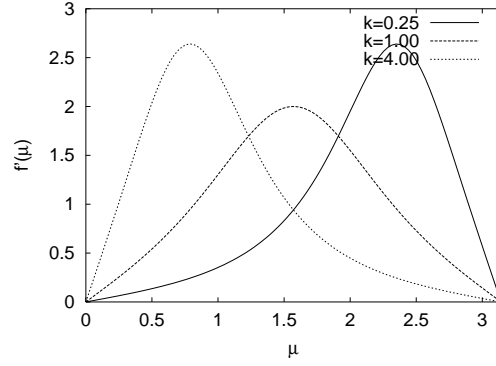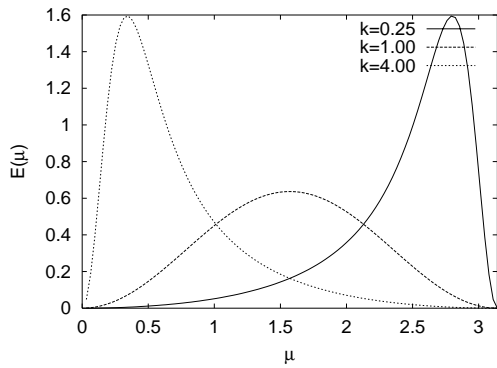
(a) $f(\mu)$ for $B = 1$
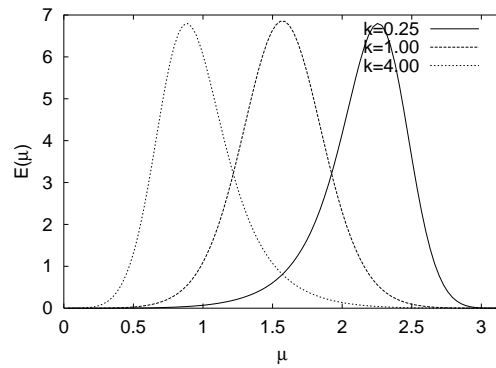
(b) $f(\mu)$ for $B = 4$

(c) $f'(\mu)$ for $B = 1$

(d) $f'(\mu)$ for $B = 4$

(e) $\tilde{E}(\mu)$ for $B = 1$

(f) $\tilde{E}(\mu)$ for $B = 4$

Figure 1: The quasi-conformal shape function $f(\mu)$, its derivative $f'(\mu)$, and the averaged energy density $\tilde{E}(\mu)$ for $B = 1$ and $B = 4$. The parameter k takes the values $\frac{1}{4}, 1, 4$.

Figure 1 shows the shape function (4.5) and its derivative for $B = N_R = 1, 4$ and for

13

$k = \frac{1}{4}, 1, 4$. Figure 1 also shows energy density $\tilde{E}(\mu)$ averaged over the 2-sphere, which is the integrand of (3.12). The shape function (4.5) has symmetry (4.7) for $k = 1$. For $k > 1$ the shape function is localized around the north pole $\mu = 0$, whereas for $k < 1$ it is localized around the south pole $\mu = \pi$. This is particularly obvious for its derivative $f'(\mu)$. Figure 1 also illustrates that for higher baryon number B the symmetric solution becomes more and more localized at the equator $\mu = \frac{\pi}{2}$. Furthermore, the energy $\tilde{E}(\mu)$ has been plotted in order to compare the result to the usual Skyrme model. $\tilde{E}(\mu)$ corresponds to an average radial density. When the energy is peaked close to $\mu = 0$ this is the usual Skyrmion. If the energy is centered around $\mu = \frac{\pi}{2}$ this corresponds to a shell-like configuration. Solutions centered around $\mu = \pi$ will correspond in the limit $L \to \infty$ to a configuration centered around infinity, with an infinite energy. In order to calculate $\tilde{E}(\mu)$ in figure 1 we have to know the values for $\mathcal{I}$ and L. As we shall see in the following, for a given B, $k \neq 1$ minimizes the energy (4.8) for a unique radius L. $k = 1$ is a solution for many different L, but among these solutions $L_{crit.}$ takes a special place. For $B = 1$, $\tilde{E}(\mu)$ has been calculated by setting $\mathcal{I} = 1$, and $L = 2.21$ corresponding to $k = 4$ and $k = \frac{1}{4}$. For $k = 1$ we have displayed $\tilde{E}(\mu)$ for the critical length $L_{crit.} = 1.41$. Similarly, for $B = 4$, $L = 2.47$ corresponds to $k = 4$ and $k = \frac{1}{4}$, and we have also displayed $\tilde{E}(\mu)$ for $L_{crit.} = 2.09$. $\mathcal{I}$ takes the value $\mathcal{I} = 20.65$ of table 1 in the appendix.

We will now discuss the energy (4.8) as a function of L. For $B = 1$, and hence $N_R = 1$, the rational map is the identity map $R(z) = z$. The integral (3.13) can be evaluated explicitly. We obtain $\mathcal{I} = 1$ so that the energy (4.8) is

$$E = 12\pi^2 \left(\frac{2L}{k + \frac{1}{k} + 2} + \frac{1}{4L} \left(k + \frac{1}{k} \right) \right). \tag{4.11}$$

It is convenient to set $\alpha = k + \frac{1}{k}$ and to calculate the minimum of the energy with respect to α. E has a single minimum at $\alpha_0 = \sqrt{8}L - 2$. For $L < \sqrt{2}$, α_0 is not attainable for real k, so that the minimum energy occurs at $\alpha = 2$ and $k = 1$. In fact, up to a minus sign this is the identity map between the physical S_L^3 and the target S_1^3. The energy E can now be written as

$$E = 6\pi^2 \left(L + \frac{1}{L} \right). \tag{4.12}$$

For $L > \sqrt{2}$ the minimum occurs where

$$k + \frac{1}{k} = \sqrt{8}L - 2. \tag{4.13}$$

Equation (4.13) has two solutions. They are related by the symmetry (3.15) and correspond to solutions localized at one of the poles. Their energy is

$$E = 12\pi^2 \left(\sqrt{2} - \frac{1}{2L} \right) \tag{4.14}$$

which is lower than (4.12). In the limit $L \to \infty$ the energy becomes $E = 12\pi^2\sqrt{2}$, and the shape function turns into $f(r) = 2\arctan(\sqrt{8}r)$ where $r = L\mu$.

Figure 2 shows the energy E of the Skyrmion as a function of L. For small L the energy scales like $\frac{1}{L}$. At the optimal value of the energy $L_{opt.} = 1$ the energy reaches its minimum $E_{opt.} = 12\pi^2$. The Skyrmion is symmetric if the radius L is below the critical radius $L_{crit.} = \sqrt{2}$. For $L > L_{crit.}$ there are two Skyrmions with the same energy. This phenomenon is often called bifurcation. There is still a symmetric solution but it is no longer stable. For $L \to \infty$ the energy tends to the $\mathbb{R}^3$ value. For $B > 1$ the energy E shows similar behaviour. The values $L_{opt.}$, $L_{crit.}$ and $E_{opt.}$ depend on the baryon number B and are good numbers to characterize the behaviour of the solutions.
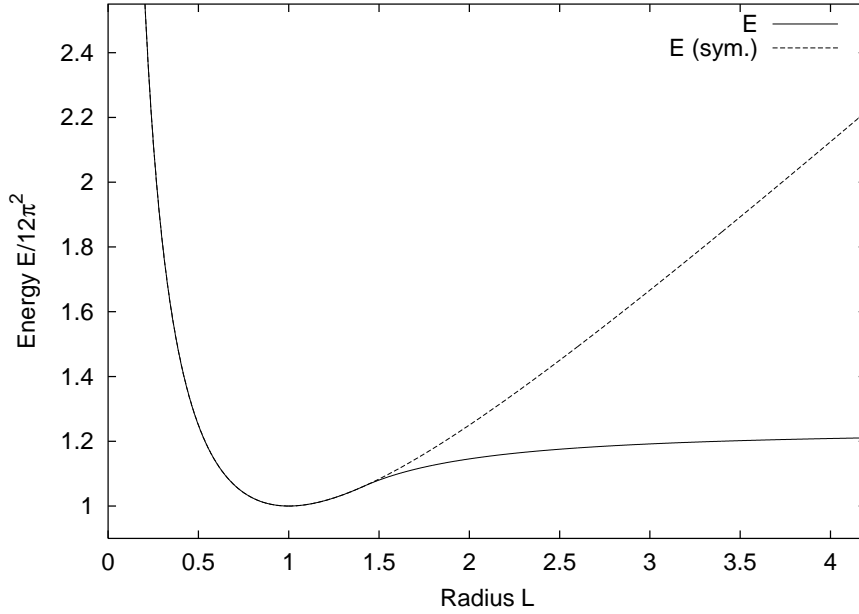

Figure 2: The energy E in units of $12\pi^2$ of a $B = 1$ Skyrmion as a function of the radius L.

Now, we consider $N_R = 4$. In this case the optimal rational map has octahedral symmetry and can be written in the following form:

$$R(z) = \frac{z^4 + 2\sqrt{3}iz^2 + 1}{z^4 - 2\sqrt{3}iz^2 + 1}. \tag{4.15}$$

We obtain $\mathcal{I} \approx 20.65$. Using expression (4.8) the energy is

$$E = \frac{24\pi^2\sqrt{2}L(\beta^3 - 6\beta + 4\sqrt{2})}{(\beta^2 - 2)^2} + \frac{5\sqrt{2}\pi^2(32 + \mathcal{I})\beta}{16L} \tag{4.16}$$

where $\beta = \sqrt{k} + \frac{1}{\sqrt{k}}$ plays the same role as α for $B = 1$. We can now minimize the energy with respect to β. This gives rise to the cubic equation

$$(\beta - \sqrt{2})^3 - P(\beta - \sqrt{2}) - Q = 0, \tag{4.17}$$

15

where $P = \frac{384L^2}{5(32+\mathcal{I})}$ and $Q = \frac{768\sqrt{2}L^2}{5(32+\mathcal{I})}$. There is a real solution β_0 for all L but its exact form is long and not very illuminating. For $L < L_{crit.}$ we have $\beta_0 < 2$ so that $\beta = 2$ and $k = 1$ is again the minimum, and the solution is localized around the equator. The critical length can be calculated by substituting $\beta = 2$ into equation (4.17), and we obtain

$$L_{crit.} = \frac{1}{24}\sqrt{\frac{15(32+\mathcal{I})}{8\sqrt{2}-11}} \approx 2.091 \tag{4.18}$$

For $k = 1$ the energy simplifies:

$$E = 24\pi^2 L(2 - \sqrt{2}) + \frac{5\sqrt{2}\pi^2(32+\mathcal{I})}{8L}. \tag{4.19}$$

The optimal length can be calculated by minimizing E with respect to L:

$$L_{opt.} = \sqrt{\frac{5\sqrt{2}(32+\mathcal{I})}{192(2-\sqrt{2})}} \approx 1.819. \tag{4.20}$$

For $L > L_{crit.}$ there are two solution such that $\sqrt{k} + \frac{1}{\sqrt{k}} = \beta_0$ related by the symmetry (3.15). The corresponding expression for the energy can be derived explicitly by setting $\beta = \beta_0$ in equation (4.16) but it is rather lengthy.

The limit $L \to \infty$ can be derived from equation (4.17). We are interested in the solution where β is of order L such that the energy E in equation (4.16) is finite. Therefore, we can neglect the last term in (4.17), and the $\sqrt{2}$, and obtain $\beta = \sqrt{P}$. Inserting β into the expression for the energy (4.16) we obtain $\frac{E}{12\pi^2} = 4.684$ which corresponds to 1.171 per baryon.

For $N_R = 9$ the optimal rational map has D_{4d} symmetry and $\mathcal{I} \approx 109.3$. It is again possible to introduce an auxiliary variable $\gamma = k^{\frac{1}{3}} + k^{-\frac{1}{3}}$. However, minimizing the energy leads to a polynomial of degree 5 in γ. Therefore it is no longer possible to calculate the solution explicitly. But the general behaviour remains the same. The solution is symmetric below a critical length $L_{crit.}$ which is determined by substituting $\gamma = 2$ into the equation for minimizing the energy. We obtain

$$L_{crit.} = \frac{2}{513}\sqrt{323190 + 1195\,\mathcal{I}} \approx 2.887. \tag{4.21}$$

The optimal radius can also be calculated analytically:

$$L_{opt.} = \frac{1}{297}\sqrt{374220 + 2310\,\mathcal{I}} \approx 2.683. \tag{4.22}$$

For $L > L_{crit.}$ there are again two degenerate solutions. In the limit $L \to \infty$ we can balance the terms which are of highest order in L. This leads to $\gamma \approx 0.779L$, and the normalized energy is $\frac{E}{12\pi^2} = 10.274$ which is 1.142 per baryon.

In the last part of this section we will discuss the limit $L \to \infty$ for general N_R. Setting $r = L\mu$ the quasi-conformal ansatz (4.5) tends to

$$f(r) = \pi - 2\arctan\left(\left(\frac{r}{R_0}\right)^{\sqrt{N_R}}\right) \tag{4.23}$$

where R_0 is a free parameter. The energy can be written as

$$E = \frac{4}{3\pi}\left(\frac{3N_R}{R_0}I_1 + \left(2N_R^2 + \mathcal{I}\right)R_0 I_2\right) \tag{4.24}$$

However, now the integrals I_1 and I_2 are independent of R_0 and depend only on N_R:

$$I_1 = \int_0^\infty \frac{r^{2\sqrt{N_R}}}{(1 + r^{2\sqrt{N_R}})^2}\mathrm{d}r \tag{4.25}$$

$$I_2 = \int_0^\infty \frac{r^{4\sqrt{N_R}}}{r^2(1 + r^{2\sqrt{N_R}})^4}\mathrm{d}r \tag{4.26}$$

It is straightforward to minimize the energy (4.24) with respect to R_0. In figure 6 and 7, in the following section we have evaluated the minimal energy $E(R_0 = R_{0,min})$, and the optimal radius $R_{0,min}$, respectively. The parameter $R_{0,min}$ has a natural interpretation as the size of the Skyrmion: For $r = R_{0,min}$ the shape function $f(r)$ has reached the value $\frac{\pi}{2}$. Furthermore, when the baryon density is integrated over a ball of radius $R_{0,min}$, then this is just half the total baryon number:

$$\frac{2N_R}{\pi}\int_0^{\frac{\pi}{2}}\sin^2 f\,\mathrm{d}f = \frac{B}{2}. \tag{4.27}$$

It is also worth noting that equations (4.5) for $k = 1$ and (4.23) are related by $r = R_{0,min}\tan\frac{\mu}{2}$. This is a stereographic projection from a 3-sphere of radius $R_{0,min}$ to $\mathbb{R}^3$. Minimizing the energy we see that a Skyrmion in flat space is related to a Skyrmion on the 3-sphere with an optimal radius $L_{opt.}$.

5 Numerical Results

In this section we discuss the numerical solution of equation (3.14) for the shape function $f(\mu)$ of the rational map ansatz and the properties of the resulting fields, and we compare it to the analytical solutions from the previous section. Here, we only consider configurations with $N_f = 1$ such that $B = N_R$. A configuration with $N_f = 2$ is discussed in the following section.

The numerical solution of (3.14) is calculated using a relaxation method. For symmetric initial conditions we obtain the symmetric solution which is a saddle point for $L > L_{crit.}$. For asymmetric initial conditions we obtain the minimum energy configuration, *i.e.* the

Skyrmion. In figure 3 we compare the numerical shape function with the quasi-conformal ansatz (4.5) for $B = 4$ and $B = 9$ at the optimal radius $L = L_{opt.}$. The optimal radius $L_{opt.}$ implies $k = 1$ in the quasi-conformal ansatz. The numerical result and the quasi-conformal ansatz show good agreement, in particular in the region around the equator $\mu = \frac{\pi}{2}$. This region is most important for the energy (3.12) since both $(f'(\mu))^2$ and $\sin^2 f(\mu)$ are large for $\mu \approx \frac{\pi}{2}$. Near the poles the numerical solution is less steep than the quasi-conformal ansatz as we expect from their exponents: $\rho_+ > \sqrt{B}$.
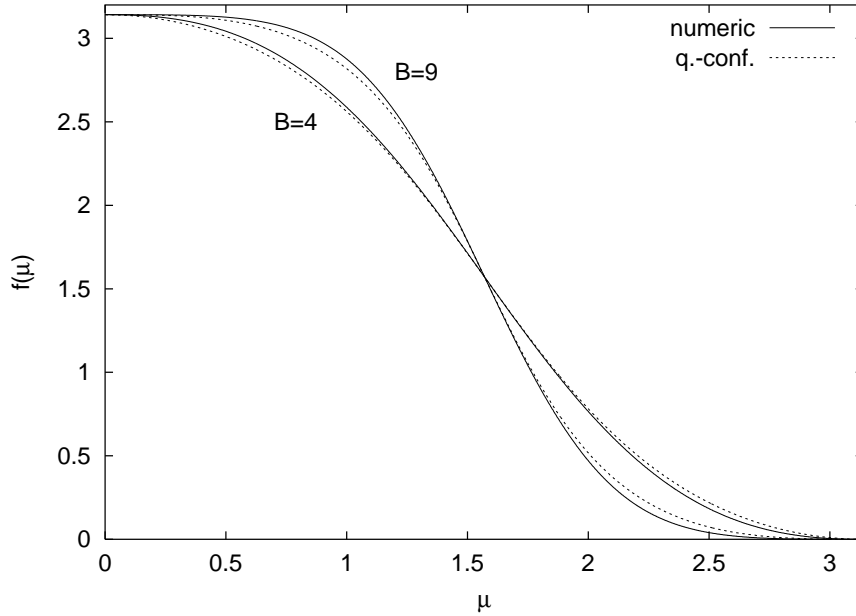

Figure 3: Comparison of the numerical shape function with the quasi-conformal ansatz for $B = 4$ and $B = 9$.

In figure 4 we show the energy E as a function of L for $B = 1, \ldots, 4$ and compare it to our analytic calculations of the previous section. In all the figures the energy E is normalized by $12\pi^2$ so that the Faddeev-Bogomolny bound (2.8) is equal to $|B|$. For $B = 1$ we plot energy (4.12) of the symmetric solution which gives the exact result. For $L > L_{crit.} = \sqrt{2}$ we also plot the energy (4.14). Our ansatz predicts the correct critical radius but energy (4.14) is slightly too high. For $B = 2$ and $B = 3$ we only display the energies of the symmetric solutions using formula (4.8) and setting $k = 1$. The integrals $I_1(1)$ and $I_2(1)$ in (4.8) are calculated numerically. Again there is very good agreement for small L, and for $L > L_{crit.}$ the ansatz is also very close to the symmetric solution. For $B = 4$ we plot the analytic expression for the symmetric solution (4.19). For $L > L_{crit.}^{q.-conf.} \approx 2.09$ we also plot (4.16) with $\beta = \beta_0$. The critical radius $L_{crit.}^{q.-conf.}$ is slightly higher than $L_{crit.}^{numeric} = 2.071$, and the energy is also slightly too high. In figure 4 we also mark the minimal energy $E_{opt.}^{numeric}$ for the optimal radius $L_{opt.}^{numeric}$ and for comparison the optimal energy $E_{opt.}^{O(2)}$ for the doubly axially-symmetric ansatz at its optimal radius $L_{opt.}^{O(2)}$. We will

18

discuss these quantities in figure 5.

In summary, all the analytical results are in good agreement with the numerical solution for a large range of L. This is quite remarkable given that the ansatz for the shape function only depends on one parameter k.
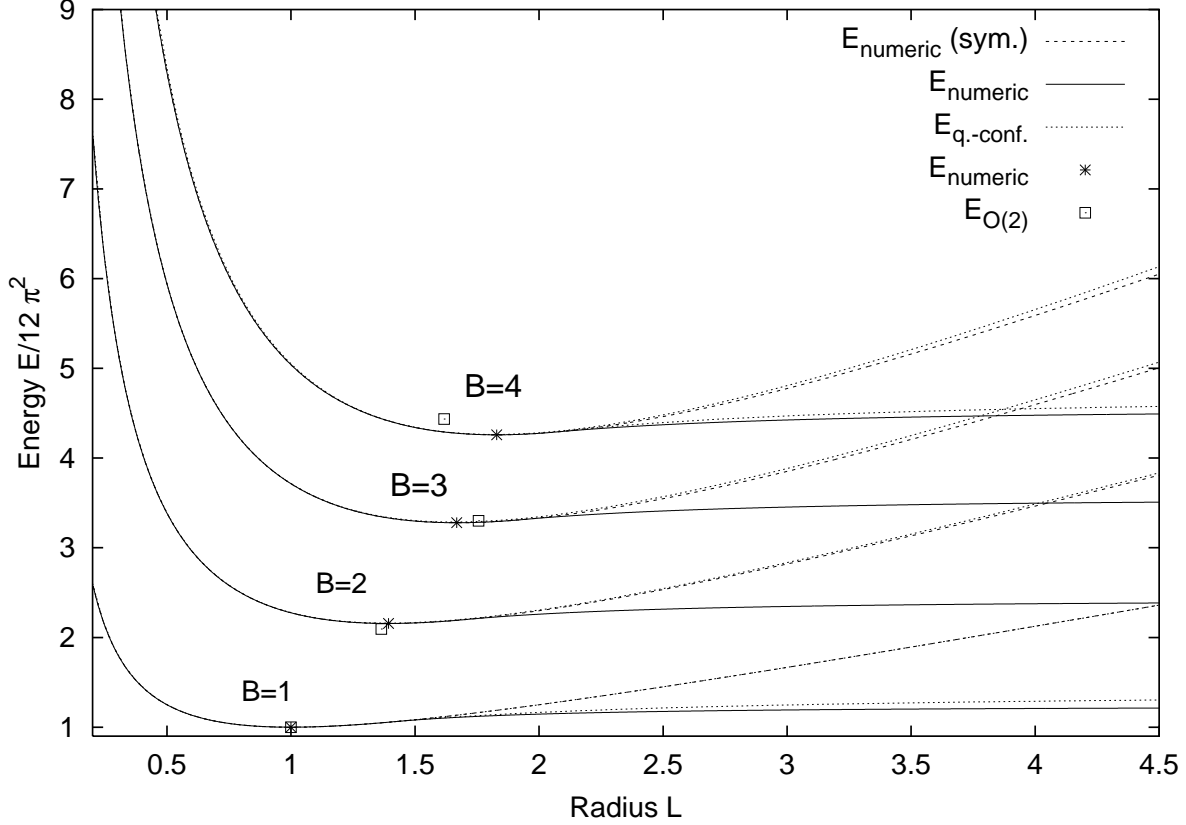

Figure 4: Comparison of the numerical calculation and the quasi-conformal ansatz for the energy E as a function of the radius L for baryon number $B = 1, \ldots, 4$.

In figure 5 we compare the optimal energy of the quasi-conformal map $E_{opt.}^{q.-conf.}$ with the energy of the doubly axially-symmetric ansatz $E_{opt.}^{O(2)}$ for all baryon numbers $B = 1, \ldots, 9$. For $B = 1$ both reproduce the exact result. For $B = 2$ the doubly axially-symmetric ansatz is believed to be the exact solution because its symmetry is compatible with the results in flat space. Yet, for $B > 2$ the energy $E_{opt.}^{q.-conf.}$ is lower than $E_{opt.}^{O(2)}$.

Figure 5 also shows that the quasi-conformal ansatz always has a lower energy than the numerical solution in $\mathbb{R}^3$. We conclude that $L_{opt.}$ for the exact solution will be finite. The horizontal line at $E = 1.232$ in figure 5 corresponds to B well separated single Skyrmions. For $B \geq 8$ the energy of the doubly axially-symmetric ansatz is above this line which is unphysical. Note that the energy per baryon in flat space $E_{\mathbb{R}^3}$ decreases as we increase the baryon number. We would obtain a similar behaviour if we kept the radius L fixed. Yet,
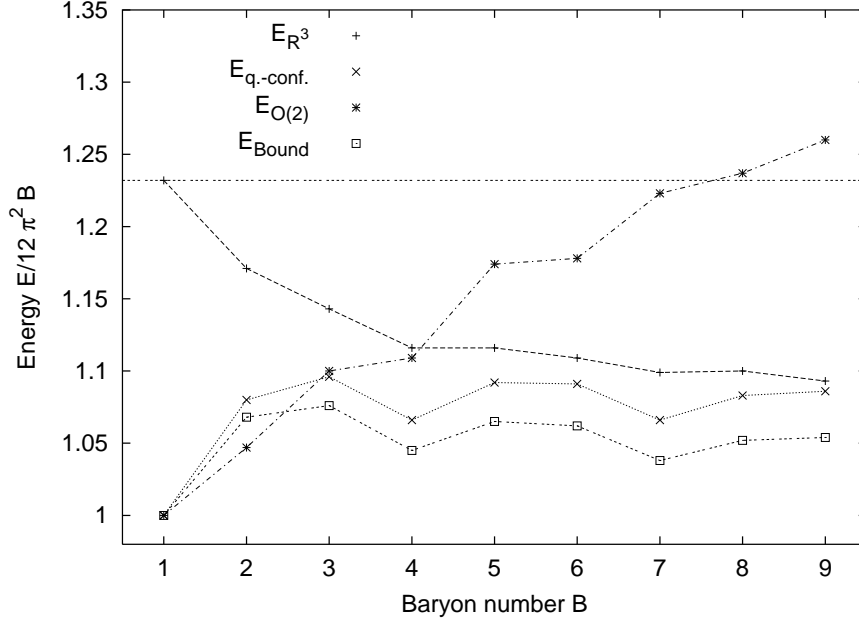
Figure 5: The energies $E^{q.-conf.}_{opt.}$, $E^{O(2)}_{opt.}$, $E_{\mathbb{R}^3}$ and E_{Bound} per baryon as a function of the baryon number B.

we then have to make the radius L large enough so that the largest Skyrmion "fits". The physical interpretation is that one multi-Skyrmion is more stable than a number of smaller Skyrmions.

We also display the rational map bound E_{Bound} (3.17). For $B = 2$ the energy of the doubly axially-symmetric ansatz is lower than E_{Bound}. This confirms our warning that energies of exact solutions do not have to be greater than E_{Bound}. However, figure 5 shows that the bound follows the general behaviour of $E^{q.-conf.}_{opt.}$ and also of $E_{\mathbb{R}^3}$.

In figure 6 we compare the energy of the quasi-conformal map $E^{q.-conf.}_{opt.}$ in the limit $L \to \infty$ to the rational map energies $E^{numeric}_{opt.}$ and the energy $E_{\mathbb{R}^3}$ of the exact solution in flat space. $E^{q.-conf.}_{opt.}$ is calculated by minimizing the energy of expression (4.24) with respect to R_0. For $B = 1, 4, 9$ the energy $E^{q.-conf.}_{opt.}$ agrees with the results of section 4. Figure 6 shows that the quasi-conformal ansatz approximates the numerical solution well. The relative difference between $E^{q.-conf.}_{opt.}$ and $E^{numeric}_{opt.}$ is monotonically decreasing and is less than 3% for $B = 4$. This means that the error of the rational map ansatz with a numerical shape function and the quasi-conformal map ansatz are of the same order of magnitude.

In figure 7 we compare the different optimal radii. The optimal radius of the quasi-conformal ansatz $L^{q.-conf.}_{opt.}$ is always slightly smaller than $L^{numeric}_{opt.}$. In all cases the value of the critical radius $L_{crit.}$ is greater than the optimal radius so that the results are consistent. The critical radius can be calculated in two different ways. In the first approach we determine the point at which the solution bifurcates. We use the fact that the symmet-
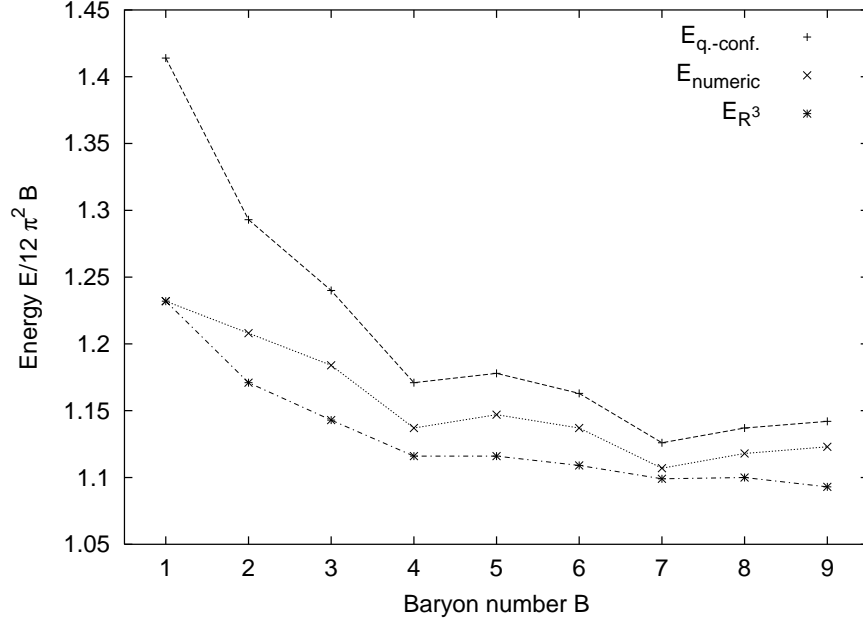
Figure 6: The energy $E_{\mathbb{R}^3}$ and the energies $E_{opt.}^{q.-conf.}$ and $E_{opt.}^{numeric}$ per baryon for $L \to \infty$ as a function of B.
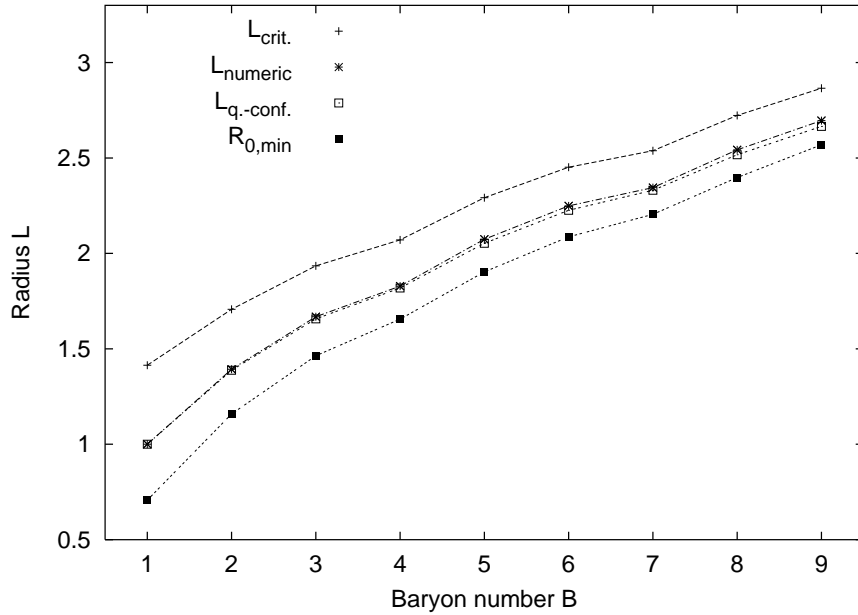

Figure 7: The radii $L_{opt.}^{numeric}$, $L_{opt.}^{q.-conf.}$, $L_{crit.}$, and $R_{0,min}$ as a function of the baryon number B.

ric initial condition relaxes into the symmetric solution which is always present, whereas an asymmetric initial condition only relaxes to the symmetric solution when there is no asymmetric solution. This method leads to rather large error bars because it is difficult to decide whether two numerically calculated solutions are different. The second approach is to consider the value of the following integral:

$$\int_0^\pi \left(f(\mu) + f(\pi - \mu) - \pi\right)^2 \mathrm{d}\mu. \tag{5.1}$$

This integral is zero if the solution possesses the symmetry (3.15) and is nonzero otherwise. We determine the value of L where the integral (5.1) first becomes nonzero. Both approaches give the same results, but the second one is much more accurate. At the critical value there is a jump in the value of the integral (5.1). This is also a verification of our analytic result that the solution is symmetric for $L < L_{crit.}$. As mentioned before, for $B = 1$ the critical radius is in agreement with the analytic result $L_{crit.} = \sqrt{2}$. For $B = 4$ the critical value of the quasi-conformal ansatz $L_{crit.}^{q.-conf.} = 2.091$ in (4.18) is only slightly higher than the critical radius of the rational map $L_{crit.}^{numeric} = 2.071$. Similarly, for $B = 9$ we calculated $L_{crit.}^{q.-conf.} = 2.887$ in (4.21) whereas $L_{crit.}^{numeric} = 2.866$.

In figure 7 we also find that $R_{0,min}$ is always smaller than $L_{opt.}^{q.-conf.}$. The difference between these lengths becomes smaller the larger the baryon number is. This confirms our interpretation stated at the end of the previous section, that the Skyrmion in flat space is related to the Skyrmion on a 3-sphere with optimal radius.

6 Phase Transitions

In this section we will describe phase transitions on S^3 as L is varied. There is no numerical work solving the full set of coupled partial differential equations for S_L^3 as there is in flat space. Therefore, we have to rely on our ansätze. First, we will discuss two different order parameters. Then we will describe particular situations in more detail.

In $\mathbb{R}^3$ the average $\langle \sigma \rangle$ is equal to 1 because of the boundary conditions at infinity. However, on S_L^3 it is easy to show that $\langle \sigma \rangle$ vanishes for $L < L_{crit.}$ when the solution is symmetric with respect to south and north pole. Therefore, we can choose $O_1 = \langle \sigma \rangle^2$ as an order parameter.[2] It has the necessary property that it is nonzero above the phase transition $L > L_{crit.}$ and identically zero below the transition. As we already pointed out in section 3 this order parameter also vanishes identically for all doubly axially-symmetric configurations. This is consistent with the fact that for $L > L_{crit.}$ these configurations are bad approximations. Another possible order parameter would be $O_2 = \langle \sigma^2 \rangle - \frac{1}{4}$. This parameter O_2 is motivated by the fact that enhanced chiral symmetry, that is a symmetry that mixes σ and π_i, could result in a vanishing of O_2.

For $B = 1$ the situation is well understood. Both parameters O_1 and O_2 vanish at the same time. Physically, this means that the localization–delocalization transition occurs at

---

[2]A more symmetric choice is $\langle \sigma \rangle^2 + \langle \pi_i \rangle^2$, [12].

the same time as the restoration of chiral symmetry [8]. In fact, for $L < \sqrt{2}$ the solution possesses full chiral symmetry $SO(4)$. For $B > 1$ the chiral symmetry will be a subgroup of $SO(4)$.

Next we discuss $B = 4$ and use both the rational map ansatz and the doubly axially-symmetric ansatz. In figure 8(a) we plot their energies. For $L > L_{crit.}$ the Skyrmion is localized at one of the poles. For smaller L the Skyrmion is localized around the equator. This is the first phase transition and the order parameter is O_1. However, there is a radius $L_{crit.'}$ where the doubly axially-symmetric ansatz with $p = 2$ and $q = 2$ becomes the minimal energy solution. As pointed out in section 3 if $p = q$ the solutions have the symmetry (3.25). For this special case we checked numerically that the symmetry is actually a symmetry of the shape function $g(\chi)$:

$$g(\chi) = \frac{\pi}{2} - g\left(\frac{\pi}{2} - \chi\right) \tag{6.1}$$

This gives rise to a symmetry between σ and π_1 and leads to the vanishing of the order parameter O_2. Therefore, we have a second phase transition at $L = L_{crit.'}$.
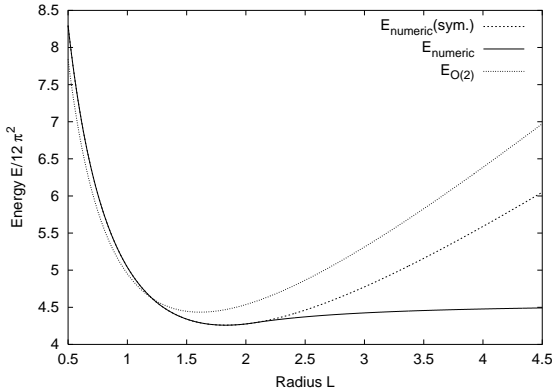
(a) The energy of $B = 4$ Skyrmions with the rational map ansatz and with the doubly axially-symmetric ansatz.
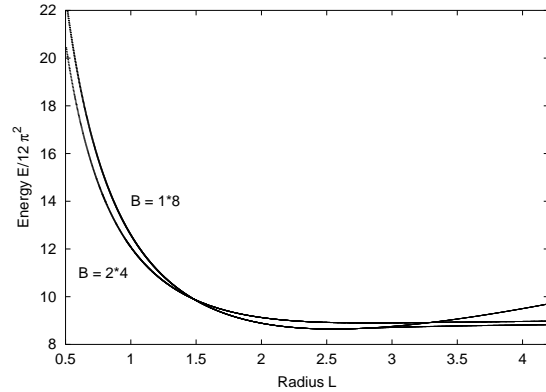
(b) The energy of two $B = 8$ Skyrmions, one with $N_f = 1$ and one with $N_f = 2$.

Figure 8: Phase transitions in the Skyrme model

As a last example we describe a Skyrmion with baryon number $B = 8$. For large L the $N_f = 1$ solution has minimal energy. However, there is a saddle point solution where two $B = 4$ Skyrmions are located at opposite poles of the 3-sphere. If L is sufficiently small there is a solution with $N_f = 2$ which has lower energy than the one with $N_f = 1$ as shown in figure 8(b).[3] This configuration is particularly interesting because both $B = 4$

---

[3]Table 2 in the appendix gives an indication when to expect a configuration with $N_f > 1$ to be more stable than the corresponding configuration with $N_f = 1$.

Skyrmions have cubic symmetry. For sufficiently small radius L_{hc} these two Skyrmions could combine and form a solution with a hypercubic symmetry. This symmetry would be strong enough to restore the symmetry between the σ- and π_i-fields. The order parameter O_2 would vanish. In this scenario there would be a localization–delocalization transition at $L_{crit.}$, whereas the chiral symmetry is further enhanced at L_{hc}. Unfortunately, these discrete subgroups of the full $SO(4)$ symmetry cannot be studied with the rational map ansatz.

In physical terms we propose the following picture. Reducing the radius L increases the baryon density. If we start with a $B > 1$ Skyrmion at large length this is well described by the rational map ansatz. There is a phase transition at the critical radius $L_{crit.}$ where the Skyrmion becomes delocalized over the 3-sphere and the order parameter O_1 vanishes. Then, one or more phase transitions follow which make the configuration more and more symmetric, and chiral symmetry is partially restored. Note however, the Skyrme model is an effective theory which is only valid for low energies. If the radius is too small we expect that further terms in the effective action become physically important.

7 Conclusion

In this paper we have described the rational map ansatz applied to Skyrmions on a 3-sphere of radius L. We have calculated the energy E of a Skyrmion as a function of L for baryon number $B = 1, \ldots, 9$ and found the following behaviour: For small L the energy E scales like $\frac{1}{L}$. E has a global minimum at an optimal radius $L_{opt.}$. When the radius L is further increased there is a bifurcation point at a critical length $L_{crit.}$: below $L_{crit.}$ the Skyrmion is symmetric under reflection at the plane through the equator of S^3. Above $L_{crit.}$ there are two degenerate Skyrmions one of which is localized at the north pole whereas the other one is localized at the south pole. For $L \to \infty$ the ansatz tends to the rational map ansatz for $\mathbb{R}^3$, [7]. For $B = 1$ and $L = 1$ our ansatz reproduces the known exact solution [16]. For $B = 2$ our results are worse for small L than the doubly axially-symmetric ansatz in [12]. However, for $B > 2$ the energies of our solutions are lower than any solutions known to date, including the doubly axially-symmetric solutions.

We have also derived an analytic expression for the shape function by imposing that the metrics on the physical S^3 and on the target S^3 are conformal in an average sense. This quasi-conformal ansatz for the shape function depends only on one parameter k. By varying k we obtain very good agreement with the numerical results for a large range of L, even for flat space. It is worth noting that the relative error of the quasi-conformal ansatz decreases with increasing baryon number. We have shown that the solution is localized at the equator if $k = 1$. For $B = 1, 4, 9$ we have shown that the Skyrmion really is symmetric below a critical value L_{crit}, i.e. $k = 1$ gives the minimal energy solution.

One particular property of the quasi-conformal shape function is that it becomes more and more localized around the equator as the baryon number increases. To be more precise, the derivative of the shape function, which is connected to the baryon density, has a peak at the equator. Since this ansatz was derived with the assumption that the map between

24

the metrics is "as conformal as possible" we have found a geometric explanation of why Skyrmions on the 3-sphere are shell-like. In flat space the map cannot be conformal. However, one "half" of the Skyrmion in flat space resembles "half" a Skyrmion on a 3-sphere with optimal radius. This fits well with the observation in section 5 that the parameter $R_{0,min}$ which is a measure of the size of the Skyrmion agrees well with the optimal length $L_{opt.}^{numeric}$.

This line of thought can be carried even further. Skyrmions on the 3-sphere might be a reasonable model for nuclei, once they are quantized. The main advantage of this model is that on the 3-sphere one-loop corrections are expected to play a far less important role than in flat space. In particular, if the Skyrmion lives on the 3-sphere with the optimal radius we expect these corrections to be so small that the predictions of the Skyrme model could be compared with experiment. The main motivation for this claim are the promising results in [20] for the $B = 1$ Skyrmion on the 3-sphere, and the fact that they predict a different value for the Skyrme coupling which is in agreement with one-loop calculations performed in [3] and the Skyrme coupling therein.

Acknowledgements

Appendix

A.1 $\mathcal{I}$ for $N = 1, \ldots, 9$ and 17

Table 1 shows the minimal value of the integral $\mathcal{I}$ in equation (3.13) as a function of N_R, as has been calculated in [7]. "APPROX" is the energy of the rational map ansatz for flat space Skyrmions where the corresponding variational equation for the shape function has been solved numerically. The column "TRUE" shows the value of the energy obtained by a numerical solution of the full set of partial differential equations. The next column "SYM" shows the symmetries of the Skyrmions. The numerical solutions and the rational map ansatz give the same symmetry. Note that the respective values for $B = 9$ in table 1 are taken from [21]. There is evidence that for $B = 9$ the symmetry and the other respective values in the table are different from the ones cited in [7].

The last two columns are the optimal length $L_{opt.}$ and the optimal energy $E_{opt.}^{numerical}$ which are displayed in figure 7 and 6, respectively. As described in chapter 5, $E_{opt.}^{numerical}$ has been obtained by using the rational map of table 1 and calculating the shape function numerically.

Following [7] we also include the values for $B = 17$. In this case the solution in flat space has marginally lower energy than $E_{opt.}^{numeric}$. However, we still expect that the rational

map ansatz is a good approximation even in this situation.

N_R	$\mathcal{I}$	APPROX	TRUE	SYM	$L_{opt.}$	$E_{opt.}^{numeric}$
1	1.00	1.232	1.232	$O(3)$	1.000	1.000
2	5.81	1.208	1.171	$O(2) \times \mathbb{Z}_2$	1.393	1.078
3	13.58	1.184	1.143	T_d	1.669	1.093
4	20.65	1.137	1.116	O_h	1.829	1.065
5	35.75	1.147	1.116	D_{2d}	2.074	1.089
6	50.76	1.137	1.109	D_{4d}	2.250	1.088
7	60.87	1.107	1.099	Y_h	2.346	1.064
8	85.63	1.118	1.100	D_{6d}	2.544	1.080
9	109.3	1.098	1.093	D_{4d}	2.696	1.083
17	367.41	1.092	1.073	Y_h	3.614	1.076

Table 1: Values of $\mathcal{I}$, the energies in flat space (APPROX, TRUE), the symmetry (SYM), and the optimal length $L_{opt.}$ and energy $E_{opt.}^{numeric}$ on S^3. All values are given for baryon number $B = N_R$ for $B = 1, \ldots, 9$ and $B = 17$.

A.2 The Rational Map Bound for Different Splittings $B = N_f N_R$

In table 2 we compare the rational map bound for different N_f. As the rational map bound is just the topological bound for $N_R = 1$, we have omitted $N_R = 1$ from table 2.

(N_f, N_R)	(1,4)	(2,2)	(1,6)	(2,3)	(3,2)	(1,8)	(2,4)	(4,2)	(1,9)	(3,3)
E_{Bound}	4.181	4.274	6.375	6.457	6.410	8.418	8.363	8.547	9.541	9.685

Table 2: The value of the generalized Faddeev-Bogomolny bound (3.17) for various values of N_f and N_R.

Table 2 can be used to estimate which combination of N_f and N_R might be more stable for a given baryon number B. It turns out that for $B = 8$ the bound is lower for $N_f = 2$ than for $N_f = 1$. It is also probable that the $(N_f = 3, N_R = 2)$ Skyrmion has lower energy than the $(N_f = 2, N_R = 3)$ Skyrmion.

References

[1] T H R Skyrme 1961 A nonlinear field theory *Proc. Roy. Soc.* **A260** 127.

[2] G Adkins, C Nappi and E Witten 1983 Static properties of nucleons in the Skyrme model *Nucl. Phys.* **B228** 552.

[3] F Meier and H Walliser 1997 Quantum corrections to baryon properties in chiral soliton models *Phys. Rep.* **289** 383.

[4] R A Leese, N S Manton and B J Schroers 1995 Attractive channel Skyrmions and the deuteron *Nucl. Phys.* **B442** 228.

[5] P Irwin 2000 Zero mode quantization of multi-Skyrmions *Phys. Rev.* **D61** 114024.

[6] R A Battye and P M Sutcliffe 1997 Symmetric Skyrmions *Phys. Rev. Lett.* **79** 363.

[7] C J Houghton, N S Manton and P M Sutcliffe 1998 Rational maps, monopoles and Skyrmions *Nucl. Phys.* **B510** 507.

[8] N S Manton 1987 Geometry of Skyrmions *Commun. Math. Phys.* **111** 469.

[9] L Castillejo, P S J Jones, A D Jackson, J J M Verbaarshot, A Jackson 1989 Dense Skyrmion systems *Nucl. Phys.* **A501** 801.

[10] M Kugler, S Shtrikman 1988 A new Skyrmion crystal *Phys.Lett.* **B208** 491.

[11] M Kugler, S Shtrikman 1989 Skyrmion crystals and their symmetries *Phys. Rev.* **D40** 3421.

[12] A D Jackson, N S Manton and A Wirzba 1989 New Skyrmion solutions on a three sphere *Nucl. Phys.* **A495** 499.

[13] C J Houghton and S Krusch 2001 Folding in the Skyrme model *J. Math. Phys.* **42** 4079.

[14] J Eells and J J Sampson 1964 Harmonic mappings of Riemannian manifolds *Am. J. Math.* **86** 109.

[15] L D Faddeev 1976 Some comments on the many dimensional solitons *Lett. Math. Phys.* **1** 289.

[16] N S Manton and P J Ruback 1986 Skyrmions in flat space and curved space *Phys. Lett.* **B181** (1986) 137.

[17] S K Donaldson 1984 Nahm's equations and the classification of monopoles *Commun. Math. Phys.* **96** 387.

[18] S Jarvis 2000 A rational map for Euclidean monopoles via radial scattering *J. Reine Angew. Math* **524** 17.

[19] M Loss 1987 The Skyrme model on Riemannian manifolds *Lett. Math. Phys.* **14** 149.

[20] S-T Hong 1998 The static properties of hypersphere Skyrmions *Phys. Lett.* **B417** 211.

[21] R A Battye and P M Sutcliffe 2000 Skyrmions, fullerenes and rational maps *Rev. Math. Phys.* **14** 29.